

Theory for an order-driven disruption of the liquid state in water

Jeremy L. England^{a)}

Department of Physics, Stanford University, Stanford, California 94305, USA

Sanghyun Park and Vijay S. Pande^{b)}

Department of Chemistry, Stanford University, Stanford, California 94305, USA

(Received 13 August 2007; accepted 16 November 2007; published online 25 January 2008)

Water is known to exhibit a number of peculiar physical properties because of the strong orientational dependence of the intermolecular hydrogen bonding interactions that dominate its liquid state. Recent full-atom simulations of water in a nanolayer between graphite plates submerged in an aqueous medium have raised the possibility of a new addition to this list of peculiarities: they show that application of a strong, uniform electric field normal to and between the plates can cause a pronounced decrease in particle density, rather than the increase expected from electrostriction theory for polarizable fluids [Vaitheeswaran *et al.*, *J. Phys. Chem. B* **70**, 6629 (2005)]. However, in seeming contradiction to this result, another study that simulated a range of similar systems has reported a less surprising electrostrictive increase in particle density upon application of the field [Bratko *et al.*, *J. Am. Chem. Soc.* **129**, 2504 (2007)]. In this work, we attempt to reconcile these conflicting simulation phenomena using a statistical mechanical lattice liquid model of water in an applied field. By solving the model using mean-field theory, we show that a field-induced transition to a markedly lower-density phase such as that observed in recent simulations is possible within a certain parameter regime, but that outside of this regime, the more conventional electrostrictive result should be obtained. Upon modifying the model to treat the case of bulk water under constant pressure in an applied field, we predict a density drop with rising field, and subsequently observe the predicted behavior in our own molecular dynamics simulations of liquid water. Our findings lead us to propose that the model considered here may be useful in a variety of contexts for describing the trade-off between orientational ordering of water molecules and their participation in the liquid phase. © 2008 American Institute of Physics. [DOI: [10.1063/1.2823129](https://doi.org/10.1063/1.2823129)]

I. INTRODUCTION

Liquid water is held together by an extensive network of relatively strong intermolecular interactions known as hydrogen bonds, which arise from the attraction between hydrogens and oxygens on adjacent molecules with suitable relative orientation.¹ Because hydrogen bonding is an orientation-dependent interaction, water can behave very differently than it does in bulk when severe confinement or some other external potential substantially constrains the rotational configurations available to the molecules of the liquid.² Exotic scenarios such as these arise frequently in contexts ranging from nanoengineering^{3,4} to macromolecular assembly,^{5,6} making the physics of ordered water a subject of both basic and practical interest in a variety of research fields.

The case of water in an applied electrostatic field provides a particularly rich setting for examining how the aqueous medium may be induced to organize itself. Water molecules possess electric dipole moments that experience aligning torques in the presence of an electric field, and these torques may find themselves at odds with the normal tendency of the liquid to arrange its orientational degrees of freedom to favor extensive hydrogen bonding. At the same

time, the capacity of each molecule of water to lower its energy by aligning its dipole with the local field produces a thermodynamic drive (known as electrostriction) to pull more molecules into regions where field is present.⁷⁻⁹ It is therefore quite challenging to make an *a priori* judgment about what the result will be when, for example, a nanolayer of water between graphite plates immersed in a water bath is subjected to a strong electric field normal to the plates.

In fact, different attempts to study such a system in simulation have led to diametrically opposite outcomes. Vaitheeswaran *et al.* used NPT molecular dynamics simulations of plates immersed in a water box to test fields ranging from 1 to 8 V per nanometer for a plate separation of roughly 1 nm, and observed an abrupt transition to approximately 50% lower particle density between the plates near 3 V/nm.¹⁰ This transition was characterized by a sharp spike in the water's compressibility, which exhibited a sustained increase relative to bulk at field strengths above the transition point. Water between the plates after the transition also was highly polarized, with most molecular dipoles making a relatively small angle with the applied field. Thus, there appeared to be a field-induced, first-order-like transition from the bulk liquid phase to an aligned phase with much lower density. In contrast, Bratko and Luzar implemented grand canonical Monte Carlo sampling of water in the region between plates of comparable separation and found for fields of

^{a)}Electronic mail: jengland@stanford.edu

^{b)}Electronic mail: pande@stanford.edu

both plate-normal and plate-parallel orientations ranging up to 4 V/nm in strength that the electric field caused the particle density between the plates to increase.¹¹

In this study, we propose a grand canonical lattice liquid model of water¹² in the presence of an organizing external field. By solving the model in the mean-field approximation, we demonstrate that it provides a consistent explanation of the results of both sets of simulations described above, which most likely differ because they are carried out in effectively distinct parameter regimes. Following this, we use our model to examine in more detail the role played by the graphite plates in helping to bring about the field-induced first-order density transition described by the theory. Finally, we augment our model to treat the isobaric-isothermal ensemble, and predict a similar density-field relationship for water in an applied field. We subsequently validate this prediction with our own molecular dynamics simulations of water at constant temperature and pressure.

II. MODEL

Our aim is to develop a statistical mechanical theory of liquid water on a discrete lattice. The fundamental physical assumption on which our model rests is that when neighboring water molecules become aligned with an applied electric field, their attempts to form hydrogen bonds with each other are frustrated by the loss of relative orientational freedom. It is this field-induced frustration of normal liquid interactions that underpins the phase transition that the model will enable us to describe.

A. Bulk mean-field theory

We begin by considering a bulk medium composed of M lattice sites, each with q neighbors, and assuming that each site on the lattice may adopt one of three different states. The first state is the e state, or “empty” state, which corresponds to the volume element represented by the lattice site not being occupied by a water molecule. The second state is the a state, or the “aligned” state, which corresponds to the site containing a water molecule with low orientational entropy that keeps its dipole moment closely aligned with the applied electric field. Finally, a site may be in an ℓ state, or “liquid” state, which obtains when the site is occupied by a water molecule that freely tumbles so as to most favorably hydrogen bond with its neighbors.

With the states for the system defined, the next step is to construct a Hamiltonian that adequately reflects the physics of the system we intend to describe. The starting point is to assume that e states, which constitute the inert vacuum against which other states are measured, do not contribute to the energy in any way. Next, we assume that an ℓ state forms in our grand canonical ensemble with chemical potential $\mu < 0$ (since the solvation free energy of water in water is exoergonic), and that it couples to neighboring ℓ states with a bonding energy $-\epsilon < 0$. The quantity ϵ reflects the total pairwise free energy of two neighboring molecules free to tumble and favorably co-orient so as to hydrogen bond with each other. We similarly require that the a state forms with chemical potential μ , but also contributes a favorable free

energy $-\gamma = h + f$, which is the sum of the enthalpy $h < 0$ of alignment with the applied field and the orientational free energy cost $f > 0$ from the reduction in entropy that accompanies alignment.

The crucial, final specification is that a states do not couple to their neighbors on the lattice, either favorably or unfavorably. This assumption is an idealization for the purpose of analytical simplicity, and it is important to discuss its justification. We reason that, although water molecules with fixed orientation do, in fact, form hydrogen bonds with neighboring water molecules, the free energy of this interaction is necessarily less favorable than that between two ℓ state molecules, since a molecule must substantially reduce its conformational entropy in order to hydrogen bond with a neighboring molecule whose orientation is already fixed. Thus, we treat the a - ℓ coupling as being negligible on the assumption that defining it to be finite but small would not lead to a qualitatively different outcome. Regarding the interaction between adjacent a states, it is clearly the case that parallel electric dipoles may either repel or attract each other depending on whether they are stacked horizontally or vertically. Thus, as a first approximation, our initial analysis assumes that a states do not interact with each other, although we will return to this issue later on.

In terms of the lattice fields $s_i^{(a)}$ and $s_i^{(\ell)}$, which are 1 when site i is in the a or ℓ state, respectively, and 0 otherwise, the Hamiltonian described above is

$$\mu N - \mathcal{H} = \sum_{i=1}^M [\mu s_i^{(\ell)} + (\mu + \gamma) s_i^{(a)}] + \frac{\epsilon}{2} \sum_{i,j}^{M,M} s_i^{(\ell)} s_j^{(\ell)}, \quad (1)$$

where i and j are neighbors on the lattice. To probe the thermodynamics of this model, we employ a mean-field approximation¹³ and assume that the grand potential per lattice site ω may be written in terms of the single-site probabilities for observing different lattice states, p_e , p_a , and p_ℓ ,

$$\omega = -\frac{q\epsilon}{2} p_\ell^2 - \mu p_\ell - (\mu + \gamma) p_a + \sum_{r=e,a,\ell} p_r \log p_r. \quad (2)$$

Here, we have assumed that the energies ω , ϵ , μ , and γ are given in units of $k_B T$, where T is the temperature and k_B is Boltmann's constant.

Minimizing this potential with respect to the probabilities on the constraint that $p_a + p_e + p_\ell = 1$ yields a self-consistency relation for the quantity p_ℓ ,

$$p_\ell = \frac{e^{q\epsilon p_\ell + \mu}}{1 + e^{\mu + \gamma} + e^{q\epsilon p_\ell + \mu}}. \quad (3)$$

It should be noted that, because ℓ states are the only ones that couple to their neighbors on the lattice, a solution to the one-dimensional self-consistency problem for p_ℓ immediately determines $p_e = (1 + e^{\mu + \gamma} + e^{q\epsilon p_\ell + \mu})^{-1}$ and $p_a = 1 - p_e - p_\ell$. In contrast, were the a states allowed to interact with neighboring sites, the self-consistency problem would become a significantly more unwieldy two-dimensional one.

A graphical solution to Eq. (3) is shown in Fig. 1. Since the self-consistency relation was derived by extremizing the grand potential, it is necessary in principle to plot $\omega(p_\ell)$ from Eq. (2) in order to determine which intersection points are

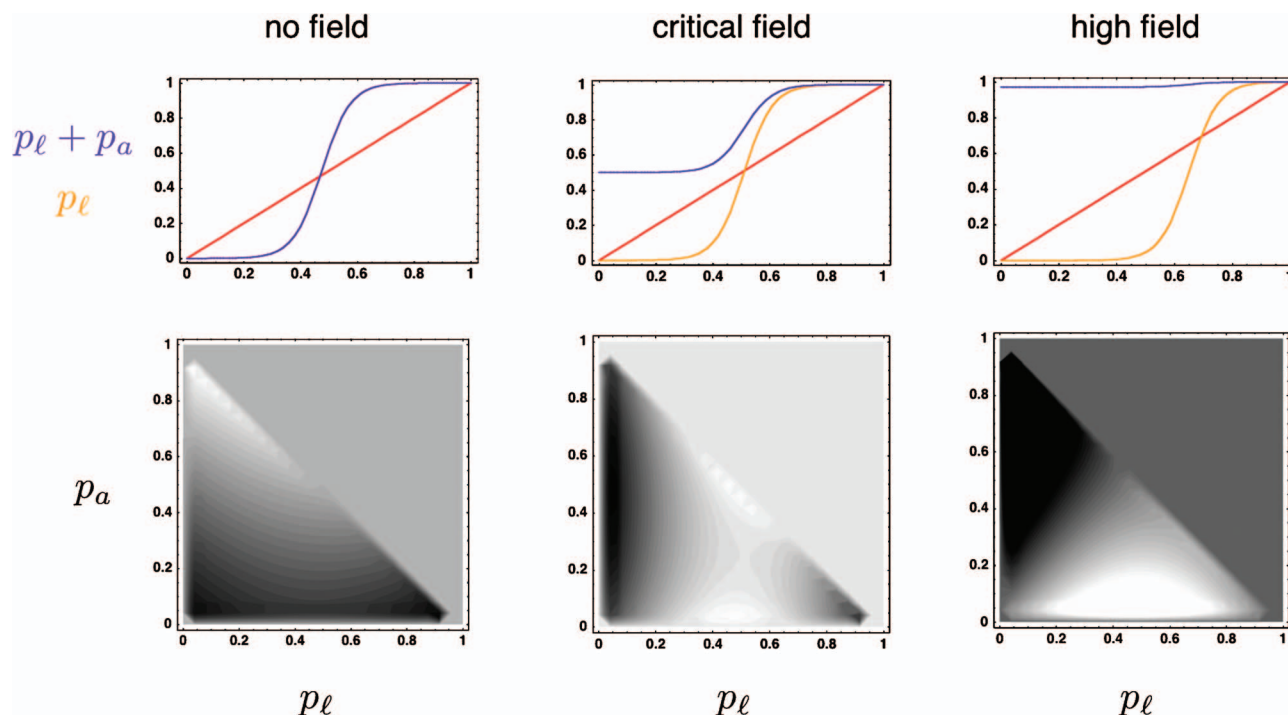


FIG. 1. (Color) Top row: Self-consistency plots are shown for p_ℓ , the probability of a site being in the liquid (ℓ) state. The left and right intersection points with the diagonal lines correspond to grand potential minima, while the central intersection is a local maximum, indicating the possibility of a first-order transition. The total particle density $p_a + p_\ell$ is also plotted. Bottom row: Grand potential contours are plotted for p_a and p_ℓ , the probability of being aligned and liquid, respectively. Shading is automatically scaled in order to make the minimum black, the maximum white, with 30 contours between and the upper half of the box shaded to match the color value of $p_\ell = p_a = 0.5$. At zero field ($\gamma = 0$) the stable global minimum lies at low p_a and high p_ℓ , which corresponds to the liquid state (left column). As the field rises, the local minimum of an aligned vapor of lower density ($p_\ell = 0$, $p_a < 1$) deepens (center column), until, at high field, it has become the global minimum (right column). In all plots, $\mu = -9.5$ and $q\epsilon = 20$.

local maxima and which are local minima, as well as which local minimum corresponds to the global minimum. We choose the parameters q , ϵ , and μ to have physically reasonable magnitude [i.e., $\mu \sim -10k_B T$ (Ref. 14) and $q\epsilon \sim 20k_B T$ (Ref. 15)], and in order that at zero field ($-\gamma = f > 0$), a liquid phase with low compressibility (Fig. 2) is stable and most

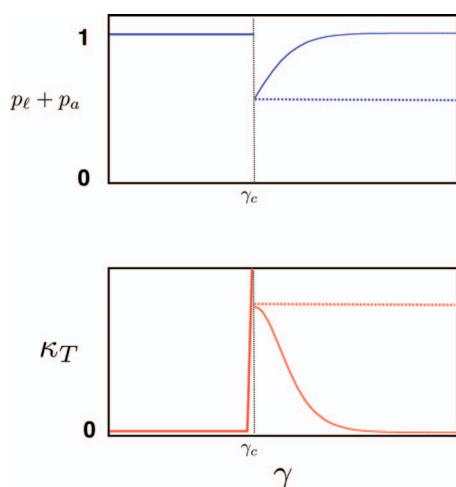


FIG. 2. (Color) Density $p_\ell + p_a$ (top) and compressibility κ_T (bottom) are plotted schematically for $\mu = -9.5$ and $q\epsilon = 20$ as a function of the applied field γ . As the critical field γ_c is reached, the density drops and the compressibility spikes. After the transition, density rises precipitously, and compressibility drops back down. Dotted lines indicate how the plots would differ if repulsion between aligned dipoles kept the density from rising so rapidly after the transition.

sites are in the ℓ state ($p_\ell \sim 1$) (Fig. 1, left panel). Here compressibility may be easily calculated from the mean-field fluctuation $\langle n^2 \rangle / \langle n \rangle^2 - 1$,¹³ where n is the number of a or ℓ states in the system. When we introduce an applied field $h < 0$, however, the relative stability of the local grand potential minimum corresponding to liquid phase decreases compared to the second local minimum near $p_\ell = 0$. Eventually, at a critical field strength where the enthalpy favoring alignment becomes greater than the enthalpic gain a molecule can realize by hydrogen bonding extensively with its neighbors ($h \sim q\epsilon$), the liquid state is destabilized, and the equilibrium begins to shift discontinuously to the second local minimum (Fig. 1, middle panel). This discontinuity in p_ℓ as a function of h corresponds to a sharp spike in the compressibility at the critical field (Fig. 2), above which the system enters a new aligned phase. For the choice of parameters used for plotting the figure, this phase has a lower density and higher compressibility than the liquid state (Fig. 2). The system therefore is capable of exhibiting a first-order phase transition that bears a striking resemblance to the one observed in previous simulations.

It nevertheless should be acknowledged that this resemblance is not exact in every detail; whereas the transition described in simulation was followed by a relatively flat dependence of particle density on the external field in the high field regime (Fig. 2, dotted curve), the solid curve shown in Fig. 2 predicts a comparatively rapid rise in density as the field ramps further past the transition point. One possible

explanation for this discrepancy is our initial failure to account for the electrostatic interaction between the molecular dipoles of adjacent water molecules. Vertically stacked parallel chains of electric dipoles attract each other, and horizontally arranged sheets of them repel each other just as strongly. For molecules in a water layer trapped between plates, vertical neighbors are less common than horizontal ones, with the result that the dipole-dipole interaction is effectively repulsive. Adding such a short-range repulsion to the theory in a Bethe-type approximation¹³ would most likely not only flatten out the post-transition density as a function of field, but would also increase the likelihood of observing a drop in density upon disruption of the liquid state.

The transition may be characterized analytically in the parameter regime we have chosen because the energy scales involved are significantly larger than $k_B T$. Because of this, the system is equivalent to an Ising model¹² (see Appendix) well below its critical temperature that chooses which ground state to be in by lowering its energy of interaction with the applied field. The grand potential per site of the liquid phase should be given by $\omega_\ell = -q\epsilon/2 - \mu$, while for the aligned phase $\omega_a = -\log[1 + e^{\mu+\gamma}]$. Setting these two quantities equal gives the critical field at which the first-order transition occurs, $\gamma_c = \log[e^{q\epsilon/2 + \mu} - 1] - \mu$. The particle density immediately after the transition follows simply as $p_a(\gamma_c) = 1 - e^{-q\epsilon/2 - \mu}$.

Interestingly, it is clear from this result that both the location of the transition point and the change in density that accompanies the transition are potentially highly sensitive to the quantity $\Delta \equiv q\epsilon/2 + \mu$. For large Δ , γ_c , and $p_a(\gamma_c)$ are both relatively flat functions. However, for $0 < \Delta \ll 1$, where the balance between the chemical potential of the bath and the binding energy of the liquid is comparatively fine, small changes in ϵ or μ of order unity can turn a dramatic density transition into a negligible one and can shift the transition point γ_c by several $k_B T$.

Armed with this observation, we are now in the position to suggest an explanation for the discrepancy between different simulations of water layers that have either increased or decreased their density upon application of a uniform electric field. The two studies were conducted in different thermodynamic ensembles, using different methods to calculate the electrostatic interactions that lead to hydrogen bonding between the water molecules. Thus, it may be the case that the two sets of simulations correspond to effective values for ϵ and μ that differ by relatively small amounts that are nevertheless qualitatively significant with respect to the question of whether a pronounced drop in density is observed at ranges of field explored. Compounding these differences is the fact that, in the study that observed an electrostrictive increase in density, the graphite plates were not modeled as hard repulsive surfaces, but rather as more physically realistic ones that exerted weak attractive forces on the water oxygens. Since it has already been established that this choice of parameters converts the sharp density transition observed in the hard repulsive case to a smoother, more moderate decline in density,¹⁰ it seems even more reasonable that a drop in density would not be observed at the relatively low fields

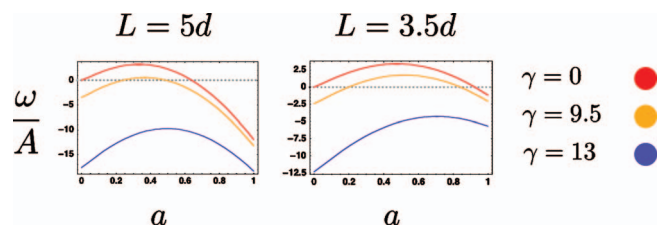


FIG. 3. (Color) Grand potential ω is plotted as a function of a , which measures the maximum value of p_ℓ for water trapped between hydrophobic plates separated by a given number of lattice spacings d . On the left, the plate separation $L=5d$ is plotted, and on the right, the result for a narrower confinement of $L=3.5d$ is plotted. Curves are drawn for no field ($\gamma=0$), moderate field ($\gamma=9.5$), and high field ($\gamma=13$). Comparing the left and right panels, it is apparent that increased confinement causes $a=0$ to become more stable than $a=1$ at a lower value of γ . Thus, narrowing of the plate separation primes the water between the plates for a field-induced partial evacuation.

considered in the Bratko study. That a moderate increase in density like the one observed in those simulations is not predicted by our model for the parameter regime in question is clearly a result of our choosing to describe each lattice site as being in one of three discrete states; in reality, one would expect liquid water to be able to act as a dielectric and polarize and pack more tightly to some degree in response to an applied field without substantially disrupting the hydrogen bond network.

B. Hydrophobic plates

Up until this point, we have analyzed our model using a zeroth-order mean-field approach that makes no distinction between different sites on the lattice. As a result, we have been unable to explicitly treat the role that the hydrophobic plates bounding the nanolayer of water may play in bringing about a phase transition. In fact, it is quite possible that these plates are essential to the process. Although our initial mean-field considerations seem to suggest that the ordering transition would be as easy to observe in bulk as in a nanoconfined system, the reality is more complicated because of long-ranged electrostatic interactions between molecular dipoles that could potentially play a dominant role in a bulk setting. In a water layer trapped between nanoseparated plates, the longest range of intermolecular interaction is limited, to the point where the nearest-neighbor approximation we employ here is better justified. Moreover, because they are hydrophobic, the plates undoubtedly contribute to disrupting the liquid state in the water layer even in the absence of field, and this destabilization may help prime the system to be pushed over the brink when the external field is turned on.

In order to assess what added effect confinement may have on the phase transition of interest, we modify our mean-field model so that the probabilities of a lattice site being in the ℓ , a , or e state are all functions of the vertical coordinate z between the plates. Thus, for a stack of lattice sheets situated between plates of separation L , the contribution to the energy of the system from ℓ - ℓ coupling is given by a sum over the z coordinate, which we may approximate with an integral if we treat $p_\ell(z)$ as a continuous function of space,

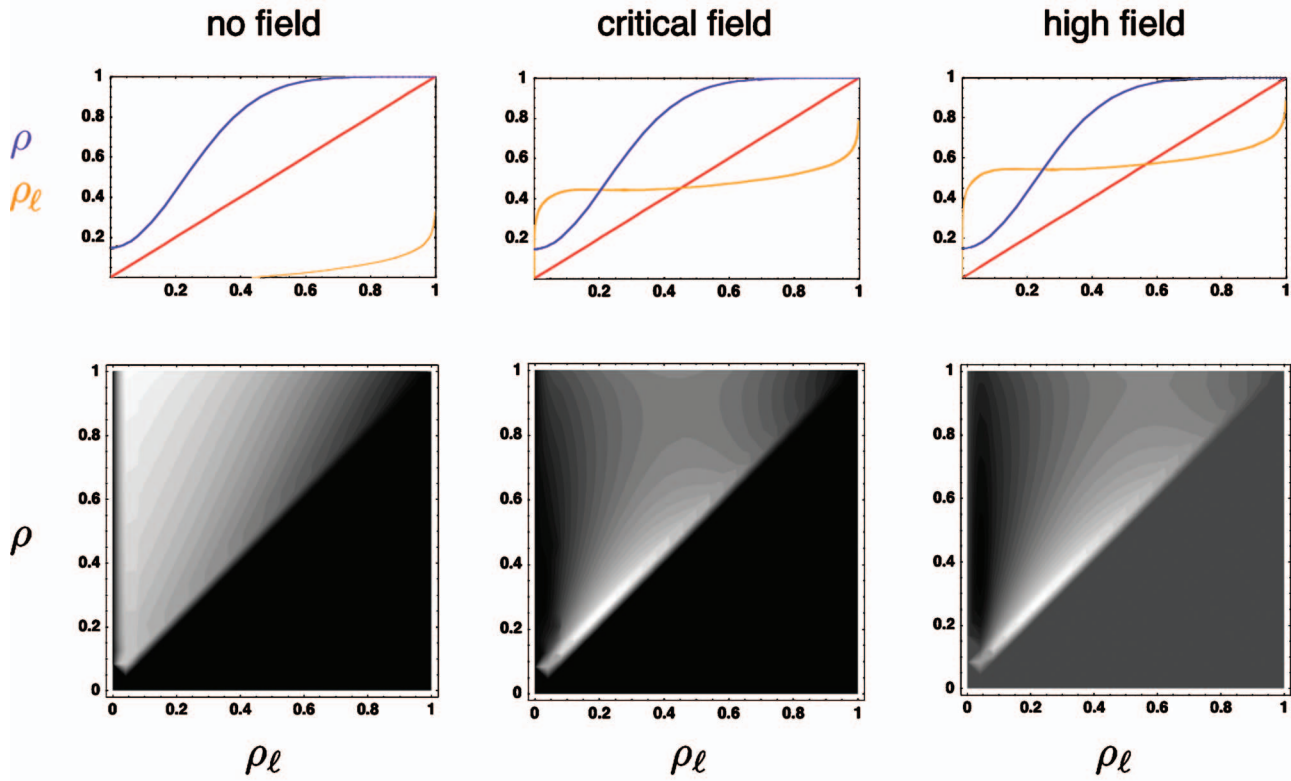


FIG. 4. (Color) Top row: Self-consistency plots are shown for ρ_ℓ , the liquid density. The left and right intersection points with the diagonal lines correspond to free energy minima, while the central intersection is a local maximum, indicating the possibility of a first-order transition. The total particle density ρ is also plotted. Bottom row: Gibbs' free energy contours are plotted for ρ and ρ_ℓ , the total and liquid density, respectively. Shading is automatically scaled so that the minimum in the field is black, the maximum white, with 25 contours in between and the lower half of the box colored to match the value of $\pi - \epsilon/2$. At zero field ($\gamma=0$) the stable global minimum lies at high $\rho \approx \rho_\ell = 1$, which corresponds to the liquid state (left column). As the field rises, the local minimum of an aligned vapor of lower density ($\rho \ll 1$, $\rho_\ell \approx 0$) deepens (center column), until, at high field, it has become the global minimum (right column). In all plots, $\pi=0.16$, the rough equivalent of 100 atm, and $q\epsilon=20$.

$$-\frac{\epsilon}{2} \sum_{z=0}^{z=L} \sum_{k=\pm 1} p_\ell(z+k)p_\ell(z) \approx -\epsilon \int_0^L dz \left[p_\ell(z)^2 + \frac{p''(z)}{2} \right]. \quad (4)$$

As before, $p_v(z)$ and $p_a(z)$ are both completely determined by the value of $p_\ell(z)$. Thus, defining $\ell(z) \equiv p_\ell(z)$, we may write the full expression for the grand potential of the system as

$$\omega = A \int_0^L dz \left[-\frac{\epsilon \ell'' \ell}{2} - \epsilon \ell^2 - (1 - p_v(\ell))\mu - p_a(\ell)\gamma + \ell \log \ell + p_v(\ell) \log p_v(\ell) + p_a(\ell) \log p_a(\ell) \right], \quad (5)$$

where A is the area of the plates.

To find the equilibrium configuration of the system, it is necessary to minimize the grand potential functional with respect to $\ell(z)$ after choosing boundary conditions that reflect the hydrophobicity of the surface (i.e., $\ell(0)=\ell(L)=0$). Rather than seek the full solution to this problem, which is likely to be intractable, we instead solve it approximately by asserting the ansatz $\ell(z)=a \sin[\pi z/L]$, where a is an undetermined parameter between 0 and 1. The rationale for assuming this form for ℓ is that the hydrophobicity of the plates should lead to a local destabilization of the liquid state near the plates that would be measured at zero field as a local

dewetting. By plugging our expression for ℓ into Eq. (5), we are able to find ω , and the equilibrium value $a=a_{eq}$ that minimizes $\omega(a)$. Thus, through our determination of a_{eq} , we are able to assay whether or not a liquid phase is stable in the region between the plates.

The grand potential as a function of a is plotted in Fig. 3 for three different values of the applied field and two different plate separations. While the separations considered are small enough (i.e., of order unity in the lattice spacing d) that the continuum approximation used here is likely to be quantitatively invalid, our expectation is that the calculation will still capture qualitative effects. For both plate configurations, sufficiently high field destabilizes the liquid state in the system and causes $\omega(a=0)$ to be more negative than $\omega(a=1)$ (blue curves). However, a comparison between the two panels demonstrates that, for a smaller separation between the hydrophobic surfaces, the unaligned liquid becomes unstable at a lower value of the applied field (orange curves). This effect results from the lesser stability at zero field of the liquid phase when it is more tightly confined between the hydrophobic plates (red curves). Thus, the plates appear to play a role in modulating the effective chemical potential of the system by pushing liquid closer to the brink of disruption, and thereby increasing its sensitivity to destabilization by the applied field.

C. Isothermal-isobaric ensemble

Thus far, we have only considered the possibility of destabilization of the liquid phase by a field in the grand canonical ensemble (GCE), where the system has the capacity to adjust the number of particles it contains. There are, however, plausible physical arguments for being able to observe a similar drop in density in a system composed of a fixed number of water molecules enclosed in a volume that can adjust itself against a constant external pressure. The underlying drive to a reduction of particle density in the GCE case is that alignment of water molecules with the applied field significantly reduces their effective attraction to their neighbors, since hydrogen bonding becomes geometrically frustrated. In a liquid at constant pressure and temperature, a reduction in the strength of the typical interparticle attraction is bound to be accompanied by an expansion in volume because the molecules no longer realize the energetic gain at higher density needed to balance the correlative entropic cost. Thus, to the extent that an applied field frustrates intermolecular hydrogen bonding in water, we expect it should push the liquid to lower density, and possibly even precipitate a first-order transition to a nonliquid phase.

In order to formalize this scenario, we envision a system with V lattice sites containing a total of $N \leq V$ particles under pressure π . For any given microstate, N_ℓ sites will be in the ℓ state, $N - N_\ell$ will be in the a state, and the rest will be empty (the e state). If we define $\rho_\ell \equiv N_\ell/V$ and $\rho \equiv N/V$, then the Gibbs free energy for the system will be given by

$$G = \frac{N}{\rho} \left[\pi - \frac{\epsilon \rho_\ell^2}{2} - \gamma(\rho - \rho_\ell) + \rho_\ell \log \rho_\ell + (\rho - \rho_\ell) \times \log(\rho - \rho_\ell) + (1 - \rho) \log(1 - \rho) \right]. \quad (6)$$

Applying the equilibrium conditions $\partial G / \partial V = 0$ and $\partial G / \partial N_\ell = 0$ yields the relationship

$$\rho = 1 - \exp[-\pi - \epsilon \rho_\ell^2 / 2], \quad (7)$$

and the transcendental equation

$$\gamma - \epsilon \rho_\ell - \log(\rho / \rho_\ell - 1) = 0, \quad (8)$$

which is solved graphically in Fig. 4. As expected, when molecules reorient in response to the rising external field, the liquid state becomes unstable and the system undergoes a first-order transition to a lower-density, field-aligned vapor phase.

As in the case of grand canonical ensemble, we can derive the location of the transition point for our system by assuming the energy scale set by the parameters in the Hamiltonian is much larger than $k_B T$. In this case, the free energy of the liquid phase is $G_\ell = N(\pi - q\epsilon/2)$, and for the aligned phase it is $G_a = N(\pi - \gamma + \log(1 - \exp[-\pi]))$. Thus, $\gamma_c = q\epsilon/2 + \log(1 - \exp[-\pi])$, and the density after the transition is $\rho = 1 - \exp[-\pi]$. For regimes in which $\pi \ll 1$ (which, at room temperature and for physically reasonable choices of ϵ and q , corresponds to pressures below roughly 10^3 atm), we may further simplify these expressions and obtain $\gamma_c = q\epsilon/2 + \log \pi$ and $\rho = \pi$.

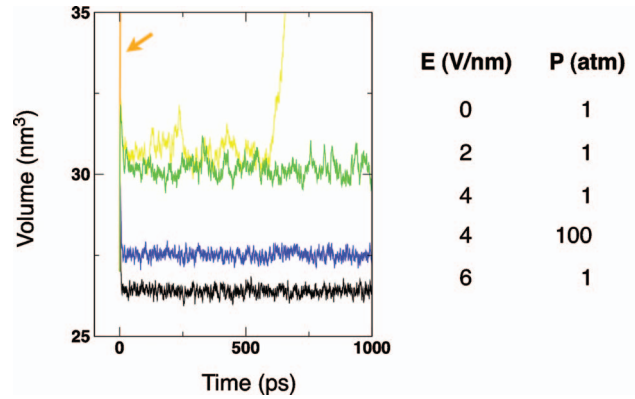


FIG. 5. (Color) Molecular dynamics trajectories of cubic water boxes initially 3 nm on a side were simulated in a uniform electric field using the GROMACS software package for 1 ns of simulation time using a time step of 2 fs. Berendsen thermo/barostats kept the system at 298 K and constant pressure (either 1 or 100 atm), respectively. A TIP4P water model was used with the AMBER2003 force-field, and 1 nm cutoff electrostatics were employed. As the applied field ramps from 0 to 2 V/nm, the specific volume increases slightly. Further increase in the field (4 V/nm) eventually leads to marginal destabilization of the liquid phase, which can be rescued by an increase in pressure from 1 to 100 atm. At high field (6 V/nm), the system immediately expands to lower density (arrow). Thus, the applied field drives a first-order transition from a high density liquid phase to a lower density aligned phase.

Intrigued by the prediction that an applied electric field might induce a pronounced drop in density for a fixed number of water molecules at constant pressure and temperature, we performed molecular dynamics simulations to see if we could observe such a transition *in silico*. Using the GROMACS software package, we ran 1 ns trajectories for initially 3 nm periodic cubes of 878 TIP4P water molecules at 298 K in different uniform external electric fields and at different pressures. The electrostatic interaction between molecules was cut off at a 1 nm range in order to isolate the issue of hydrogen bonding and avoid interference from long-range interactions between distant dipoles that might complicate the outcome outside of the nanoscale regime. The volume of the box for each field and pressure is plotted in Fig. 5 as a function of time. For low field of 2 V/nm, a moderate expansion takes place, indicating that the effective attraction between neighboring molecules has already become moderately reduced as polarization of the liquid begins to compete with hydrogen bonding (blue trace). At a field of 4 V/nm, the polarized vapor phase is marginally more stable than the liquid, and the kinetics of the transition from the starting local free energy minimum to the global one are resultingly slow enough that the expansion takes place only after roughly 500 ps (yellow trace). Consistent with our expectation from the expression we have derived for γ_c , increasing the pressure on the system at the same applied field restores the stability of the liquid state by shifting the critical field higher. Finally, at a high field of 6 V/nm, the liquid state dissipates so rapidly that the volume of the system is in free runaway for the entire trajectory (orange trace). Thus, the applied electric field is evidently capable of driving a first-order disruption of the liquid phase very much like the one predicted by mean-field theory.

III. DISCUSSION

The effects of hydrophobicity² and electrostatics¹⁶ on the organization of aqueous solvent have separately received extensive attention from analytical theorists, yet comparatively few attempts have been made to use theory to address the solvation physics of both charged and nonpolar surfaces within a single framework.^{17,18} Ironically, this outcome might be due at least in part to the success past theories have had within their own domains: a model that too effectively understands the particularities of how liquid water restructures itself in a purely hydrophobic context may lack the flexibility to accommodate a mixed scenario in which electric fields make qualitatively new and different demands on the hydrogen bond network. The importance of developing theoretical tools for treating such mixed scenarios is underlined by growing evidence from simulation that hydrophobicity and charge interact complexly when they share the same solvent environment.^{9,19–22}

In this study, our strategy has been to describe both hydrophobic and electrostatic effects so simply that the two phenomena can be captured within a single analytical formalism. The danger of this approach is obviously that we may, by simplifying matters excessively, ignore details that are crucial to the phenomena of interest. Whether or not we have fallen into this trap is an empirical question, which we sought to answer here by comparing the predictions of our theory to the results of atomistic simulations.

We began by abstracting the internal configurations of water into three different states for each molecule-sized site on a lattice. The liquid (ℓ) state was made to correspond to a freely tumbling molecule forming hydrogen bonds with its liquid neighbors, the aligned (a) state to a molecule whose energetically favorable fixed dipole orientation made it less able to interact attractively with nearby sites, and the empty (e) state to a small volume in space not occupied by a molecule. The fundamental assumption that allowed us to construct a physically reasonable Hamiltonian for this system was that the choice between participation in the liquid phase and alignment with the external field was energetically frustrated because of the orientational sensitivity of hydrogen bonds.

We first solved our theory for a grand canonical bulk medium in the mean-field approximation, and showed that as the strength of the applied field γ passes through a critical value γ_c , the system undergoes a first-order phase transition from an incompressible liquid state to a compressible aligned state whose initial density after the transition depends sensitively on the chemical potential of the bath. We thus were able to describe a transition to lower density strikingly similar to the one reported by Vaitheeswaran *et al.* in their study of water in a uniform field, while also possessing the means to suggest why a similar study performed by Bratko and Luzar recorded no field-induced density decrease: it is reasonable to hypothesize that the two simulations were effectively operating at slightly different chemical potentials and ℓ - ℓ couplings. At the same time, our theory predicted a more rapid electrostrictive increase in density with the field above the transition than was observed in the Vaitheeswaran study.

This is undoubtedly a quantitative, and not a qualitative, disagreement; it must be the case that, for high enough fields, aligned water molecules are pulled back between the plates by electrostriction, and the density resultantly increases. To the extent that Vaitheeswaran *et al.* did not observe this density rebound to occur as rapidly after the transition as our theory would predict, we propose that this discrepancy arises because we did not include a term in our Hamiltonian accounting for the electrostatic repulsion between horizontally arrayed coaligned electric dipoles that would tend to drive the aligned vapor to lower density.

Having demonstrated the efficacy of our theory in describing a phenomenon observed previously in simulation, we next modified the model to make it spatially dependent, thus enabling us to examine in closer detail the interplay between confinement of water in a hydrophobic environment and the alignment of the water molecules with an external field. We found that the degree of confinement enhanced the liquid's sensitivity to destabilization by the field. In addition, the model also predicts that, before any field-induced transition takes place, the increase in applied field will cause a shift in the equilibrium between a and e states that should be most noticeable at the plate surface, where $p_\ell=0$ and p_a+p_e is therefore maximized. It is worth noting that such a field-induced wetting at the plate surface was observed in the study of Bratko and Luzar.

Perhaps the most compelling demonstration of the utility of our model, however, was that we were able to retool it for use in a different thermodynamic ensemble. There, it predicted a similar, but distinct, first-order density drop in the presence of an applied field. After characterizing this phenomenon analytically, we showed that it occurs in molecular dynamics simulations in accordance with our expectations. It should be stressed that this result could not have been predicted merely from the equivalence of thermodynamic ensembles. As the field rises at constant chemical potential, the pressure of the system will not, in general, remain constant. To see this, we recall that the grand potential per site ω in GCE is, in fact, equal to the pressure. Thus, to whatever extent the grand potential varies with γ , the system cannot be considered isobaric. However, both the grand canonical and isobaric transitions described by our model originate from the same physics: in each case, a field-driven reduction in the conformational entropy of water molecules reduces their attraction to their neighbors, with the result that the liquid state is destabilized.

The case of an aqueous medium in a uniform electric field provides a rich setting in which to examine the statistical physics of liquid water in simulation, and yet there are several reasons to be pessimistic about the eventual experimental observation of a density transition like the one we have considered in this study. In the bulk regime, it is likely that the long range of the electrostatic interaction would significantly complicate the forces acting on the molecules in the liquid, as evidenced by the fact that when we perform simulations of water in an applied field using a particle mesh Ewald electrostatics method that accounts for long-range effects, the system contracts instead of expanding (data not shown). In the nanoregime, it is questionable whether suffi-

ciently uniform fields can be generated on the relevant length scales, making it likely that any charged surface involved would strongly bind the waters closest to it and thereby qualitatively alter the solvent organization relative to what it would be in a perfectly uniform field. It is furthermore questionable whether results of simulations carried out at such high electric field strengths can be trusted when they are performed using a nonpolarizable, nonionizable water model.

IV. CONCLUSIONS

With all of the above caveats in mind, we nevertheless would argue that the simulation phenomenon examined in this work has proved to be an excellent testing ground for our analytical theory for the ordering and depletion of water in the presence of hydrophobic surfaces and electric fields. Despite being formally quite simple (and therefore quite tractable), our model has succeeded in capturing diverse aspects of a class of phase transitions by describing the choice water molecules must make between orientational ordering and participation in the liquid phase. Water undoubtedly faces this choice in a wide variety of contexts ranging from structural biology to nanofluidics. Thus, in future work, we look forward to applying different variations on the theoretical framework laid out here to understand the ordering of water inside macromolecular assemblies and the *in vivo* folding of confined proteins.

ACKNOWLEDGMENTS

One of the authors (J.E.) thanks the Fannie and John Hertz Foundation for support. This work was also supported by NIH NIGMS (R01 GM062868) and the NIH Nanomedicine Center for Protein Folding Machinery (PN1EY016525). The authors are grateful to Professor David Chandler for helpful comments.

APPENDIX: EQUIVALENCE TO AN ISING MODEL

The Hamiltonian presented in Eq. (1) describes a lattice gas whose nonempty sites can be in one of two states: an ℓ state that couples to neighboring sites or an a state that does not. However, it is formally useful to observe instead that both the a and e states do not interact with their neighbors, and may therefore be thought of as the internal states of a two-state vacuum that reaches its own thermodynamic equilibrium, with free energy $-\log(1 + \exp[\gamma + \mu])$. Thus, summing over e and a states in the full partition function for the system, we obtain an effective Hamiltonian for a single-component lattice gas,

$$\mu N - \mathcal{H}_{eff} = (\mu - \log(1 + \exp[\gamma + \mu])) \times \sum_{i=1}^M s_i^{(\ell)} + \frac{\epsilon}{2} \sum_{i,j}^{M,M} s_i^{(\ell)} s_j^{(\ell)}. \quad (A1)$$

The system is therefore exactly equivalent to an Ising model¹² in an external field that depends nonlinearly on the applied electric field described by γ . Since we assume the liquid phase to be stable for $\gamma=0$, we know we are below the critical temperature for the system and that there should therefore be a first-order transition between liquid and vacuum phases for a critical value of γ .¹³ Moreover, it is clear that the transition point between the liquid and vacuum phases should be located where the applied field in the Ising description changes sign, since it is at this point that the symmetry between spin “up” and “down” is broken. Thus, $\gamma_c = \log[e^{q\epsilon/2 + \mu} - 1] - \mu$.

¹I. Tinoco, Jr., K. Sauer, and J. C. Wang, *Physical Chemistry* (Prentice Hall, Upper Saddle River, NJ, 2007).

²D. Chandler, *Nature (London)* **437**, 640 (2005).

³G. Hummer, J. C. Rasaiah, and J. P. Nowortya, *Nature (London)* **414**, 188 (2001).

⁴O. Byl, J. Liu, Y. Wang, W. Yim, J. K. Johnson, and J. T. Yates, *J. Am. Chem. Soc.* **128**, 12090 (2006).

⁵Y. M. Rhee, E. J. Sorin, G. Jayachandran, E. Lindahl, and V. S. Pande, *Proc. Natl. Acad. Sci. U.S.A.* **101**, 6456 (2004).

⁶P. Liu, X. Huang, R. Zhou, and B. J. Berne, *Nature (London)* **437**, 159 (2001).

⁷L. D. Landau, E. M. Lifshitz, and L. P. Pitaevski, *Electrodynamics of Continuous Media* (Butterworth-Heinemann, Oxford, 1993).

⁸J. Kirkwood and I. Oppenheim, *Chemical Thermodynamics* (McGraw-Hill, New York, 1993).

⁹J. Dzubiella and J.-P. Hansen, *J. Chem. Phys.* **119**, 12049 (2003).

¹⁰S. Vaitheeswaran, H. Yin, and J. C. Rasaiah, *J. Phys. Chem. B* **70**, 6629 (2005).

¹¹D. Bratko, C. D. Daub, K. Leung, and A. Luzar, *J. Am. Chem. Soc.* **129**, 2504 (2007).

¹²T. D. Lee and C. N. Yang, *Phys. Rev.* **87**, 410 (1952).

¹³R. Pathria, *Statistical Mechanics* (Butterworth-Heinemann, Oxford, 1996).

¹⁴M. R. Shirts and V. S. Pande, *J. Chem. Phys.* **122**, 134508 (2005).

¹⁵S. J. Suresh and V. J. Naik, *J. Chem. Phys.* **113**, 9727 (2003).

¹⁶B. Roux and T. Simonson, *Biophys. Chem.* **78**, 1 (1999).

¹⁷J. Dzubiella, J. M. J. Swanson, and J. A. McCammon, *Phys. Rev. Lett.* **96**, 087802 (2006).

¹⁸Y. Chen and J. D. Weeks, *Proc. Natl. Acad. Sci. U.S.A.* **103**, 7560 (2006).

¹⁹D. Bulone, V. Martorana, P. L. San Biagio, and M. B. Palma-Vitorelli, *Phys. Rev. E* **56**, R4939 (1997).

²⁰D. Bulone, V. Martorana, P. L. San Biagio, and M. B. Palma-Vitorelli, *Phys. Rev. E* **62**, 6799 (2000).

²¹J. Dzubiella and J.-P. Hansen, *J. Chem. Phys.* **121**, 5514 (2004).

²²S. Vaitheeswaran and D. Thirumalai, *J. Am. Chem. Soc.* **128**, 13490 (2006).